Revista Brasileira de Geografia Física v.18, n.03 (2025) 2104-2120.

ISSN:1984-2295

Revista Brasileira de Geografia Física

Homepage:https://periodicos.ufpe.br/revistas/rbgfe

Monitoring the variation in land surface temperature in a region of the Amazon biome

Karina Fragoso Hermenegildo[1], Luiz Carlos Teixeira Coelho[2], Luiara Castro de Lana[3], Mateus Ribeiro Rodriguez[4], Sonia Maria Lima Silva[5]

[1] BSc in Cartographic Engineering, Rio de Janeiro State University, Rua São Francisco Xavier, 524, sala 4044F - Maracanã, Rio de Janeiro - RJ, 20550-013, Brazil, +55 21 2334-0648, karina.fragoso@hotmail.com, https://orcid.org/0009-0000-6324-4991. [2] Dr. in Urban and Regional Planning, Professor at the Rio de Janeiro State University, Rua São Francisco Xavier, 524, sala 4044F - Maracanã, Rio de Janeiro - RJ, 20550-013, Brazil, +55 21 2334-0648, luiz.coelho@eng.uerj.br, https://orcid.org/0000-0002-4466-9772. [3] MSc. in Environmental Engineering, Rio de Janeiro State University, Rua São Francisco Xavier 524 sala 5029-F - Maracanã - RJ - Rio de Janeiro - CEP: 20550-013 – Brasil, +55 21 975370947, luiaralana@gmail.com, https://orcid.org/0000-0001-8375-5772. [4] MSc in Geography, Federal Rural University of Rio de Janeiro, Km 07, Zona Rural, BR-465, Seropédica - RJ, 23890-000, +55 21 99735-1552, mribeiro.rodriguez@gmail.com, https://orcid.org/0000-0003-3072-0431. [5] Dr. in Geography and Geology, Professor at the Rio de Janeiro State University, Rua São Francisco Xavier, 524, sala 4044F - Maracanã, Rio de Janeiro - RJ, 20550-013, Brazil, +55 21 2334-0648, sonia.silva@eng.uerj.br, https://orcid.org/0000-0002-2414-1516. (corresponding author).

Artigo recebido em 11/10/2024 e aceito em 29/01/2025

A B S T R A C T

Studying wildfires is crucial to understand the factors that influence their occurrence, enabling effective monitoring and the mitigation of their environmental impacts. The main objective of this study was to monitor the variation in land surface temperature in a region of the Amazon biome, more specifically in the municipality of Porto Velho, for the years 2015 and 2018. The secondary objectives were: calculation of spectral indices and surface temperature, identification of classes of land use and occupation maps and finally, quantification of areas in the synthetic maps of land use and occupation and surface temperature. To conclude, the results of the analysis of thematic maps and index maps showed that urbanized areas and exposed soil had a higher temperature than the other classes, indicating a correlation between temperature and land use. Furthermore, the differentiated burning index by normalized ratio (dNBR) obtained the best performance in identifying burned areas. In short, environmental degradation and the presence of asphalt surfaces also contributed to the increase in soil temperature.

Keywords: Remote Sensing. Spectral Indices. Surface Temperature. Termal Sensors.

Monitoramento da variação de temperatura de superfície terrestre em uma região do bioma Amazônia

R E S U M O

Estudar os incêndios florestais é fundamental para compreender os fatores que influenciam sua ocorrência, permitindo um monitoramento eficaz e a mitigação de seus impactos ambientais. O presente estudo teve como objetivo principal monitorar a variação de temperatura de superfície terrestre em uma região do bioma Amazônia, mais especificamente no município de Porto Velho, para os anos de 2015 e 2018. Os objetivos secundários foram: cálculo de índices espectrais e temperatura de superfície, identificação das classes de mapas de uso e ocupação do solo e por fim, quantificação das áreas nos mapas sínteses de uso e ocupação do solo e de temperatura de superfície. Para concluir, os resultados das análises dos mapas temáticos e mapas de índices mostraram que áreas urbanizadas e de solo exposto apresentaram temperatura mais elevada que as demais classes, indicando uma correlação entre a temperatura e o uso do solo. Além disso, o índice diferenciado de queima por razão normalizada (dNBR) obteve o melhor desempenho na identificação de áreas queimadas. Em suma, a degradação ambiental e a presença de superfícies com asfalto também contribuíram para o aumento da temperatura do solo.

Palavras-chave: Sensoriamento Remoto. Índices Espectrais. Temperatura de Superfície. Sensores Termais.

Introduction

Brazil is home to the greatest biodiversity in the world, represented by six distinct terrestrial biomes. These biomes consist of groups of ecosystems that share similar characteristics in terms of fauna and flora. Among them, the Amazon biome is notable for its ability to harbor a wide variety of organisms and dense, diverse vegetation. Additionally, the Amazon biome contains the largest tropical rainforest in the world, covering approximately 4,196,943 km², which accounts for more than 40 percent of the national territory. Despite the importance of this region, recurrent fires pose a significant threat, directly impacting existing biodiversity, risking the extinction of various species, and affecting the lives of the local population (Instituto Brasileiro de Florestas [IBF], 2023).

However, this region faces increasing threats, with wildfires and forest fires being one of the main problems. These events, which can have natural or anthropogenic origins, result in ecosystem degradation, putting the survival of numerous species at risk and compromising the quality of life of local populations. Additionally, fires in the Amazon contribute to the emission of greenhouse gases, intensifying global warming and the impacts of climate change. The frequency and intensity of wildfires may be influenced by a variety of factors, such as deforestation, logging, and prolonged drought periods, which are often linked to improper land use and climate change (GOMES et al, 2024; IPCC, 2024).

The main factors driving fires in the Amazon include deforestation for agricultural expansion, inadequate farming practices, illegal logging, prolonged droughts exacerbated by climate change, and land grabbing, which uses fire as a tool to "clear" forested areas. Additionally, human activities such as infrastructure development and irregular settlements often contribute to fire ignition, while forest degradation increases vulnerability to fire. The combination of these factors creates a vicious cycle that intensifies biodiversity loss, undermines ecosystem services, and worsens socio-environmental impacts in the region (Alencar, et al., 2015; Verbeke, et al., 2018; Gomes et al, 2024; Hahn et al., 2014; IPCC, 2024).

In this context, environmental monitoring becomes essential, with an emphasis on the use of technologies that allow for the assessment of the impacts of wildfires and their relationship with land use and occupation. This issue has been a significant concern for environmental scientists for two primary reasons: first, the Amazon Forest is vast, making its misuse by poachers and loggers challenging to control; second, forest fires can spread rapidly, leading to a tremendous loss of biodiversity, which is exceedingly difficult to recover.

In this context, the digital processing of remotely sensed images has emerged as a vital tool for monitoring land use changes and identifying potential sources of wildfires within days when satellite imagery is utilized. For instance, Castillo et al. (2020) effectively used medium-resolution Landsat-8 and Sentinel-2 imagery to monitor wildfires in the Peruvian Amazon. Their study employed indices such as the MIRBI (Mid-Infrared Burn Index), NBR (Normalized Burn Ratio), NBR2 (Normalized Burn Ratio 2), and NIR (Near-Infrared), along with post-fire values of these indices, to track changes and assess fire impacts.

Similarly, Santana et al. (2018) demonstrated the utility of low-resolution standardized MODIS (Moderate Resolution Imaging Spectroradiometer) time series for monitoring wildfires and deforestation in Novo Progresso, Pará. Their study utilized indices such as BAIM (Burn Area Index for MODIS), GEMI (Global Environmental Monitoring Index), MIRBI, NBR, NBR2, and NDVI (Normalized Difference Vegetation Index). Despite the lower spatial resolution of MODIS, their results aligned closely with those derived from Landsat-8 imagery, showcasing the effectiveness of consistent time series data in wildfire and land use monitoring. Nolde et al. (2021) further highlighted the consistency of remote sensing indices across different spatial resolutions by combining MODIS with other sensors in their analysis.

Burn-related indices, including NBR, NBR2, delta Normalized Burn Ratio (dNBR), and the Normalized Burn Ratio Plus (NBR+), have been successfully applied in diverse regions worldwide. Examples include studies in Eastern Australia (Nolde et al., 2021), California (Miller & Thode, 2006), Sicily (Alcaras et al., 2022), Sardinia (Costa-Saura et al., 2022), Sumatra (Mayang and Angraina, 2022) and Siberia (Delcourt et al., 2021). These studies demonstrate that normalized burn indices offer a robust solution for monitoring human activities, particularly those linked to forest clearing via fires, regardless of geographic location (van Gerrevink and Veraverbeke, 2021). When combined with traditional indices like NDVI and NDWI (Normalized Difference Water Index), these metrics provide a comprehensive view of land use over large geographic areas, aiding environmentalists and policymakers in monitoring and managing territories at risk of forest fires.

Moreover, as with many anthropogenic activities, deforestation—whether due to illegal logging or burning—tends to follow identifiable patterns that can be detected using geotechnologies. Daldegan et al. (2014) combined remote sensing imagery with Geographic Information Systems (GIS) to produce a supervised classification of fire recurrence in the Brazilian Cerrado, identifying trends in specific zones. Similarly, Reis and Leal (2020) observed comparable patterns in the Amazon, particularly in the municipality of Lábrea, Amazonas, using fire geolocation data from the PRODES (Satellite Monitoring of Amazon Deforestation) Project.

Consequently, a combined approach that integrates remotely sensed imagery with geoinformation tools is consistent with recent research for monitoring deforestation and forest fires. This study proposes utilizing a combination of indices, thermal data, and digital cartography tools to monitor surface temperature, which serves as an indicator of both forest fires and human activities.

Therefore, the main objective of this study is to monitor surface temperature variations in an area located in the Amazon biome, focusing on the municipality of Porto Velho, Rondônia. The specific objectives include calculating spectral indices and surface temperatures, identifying land use and occupation classes, and quantifying areas through synthesis maps of land use, occupation, and surface temperature. The expected results include the creation of thematic maps representing land use and occupation classes, surface temperature, and indices such as NDVI, NDWI, and NBR, as well as the quantification of areas related to the mapped classes.

By integrating these data, the study aims to provide complementary information that helps in understanding the interrelationships between spectral indices, land use and occupation classes, and surface temperature variations. This knowledge could support conservation strategies, impact mitigation, and sustainable management, contributing to the preservation of the Amazon and addressing climate change.

Based on the above, the hypothesis to be demonstrated is that there is a correlation between the results of specific spectral indices, land use and land cover classes and surface temperature.

Materials and Methods

The study area is the municipality of Porto Velho, capital of the State of Rondônia, Brazil. The municipality is located on the right bank of the Madeira River (Prefeitura de Porto Velho, 2023), a tributary of the Amazon River in the northern region of Brazil (Figure 1). The study area is part of the Amazon biome and their geographic coordinates are: latitude 8°45'48.81"S and longitude 6353'49.81"W (Instituto Brasileiro de Geografia e Estatística [IBGE], 2023).

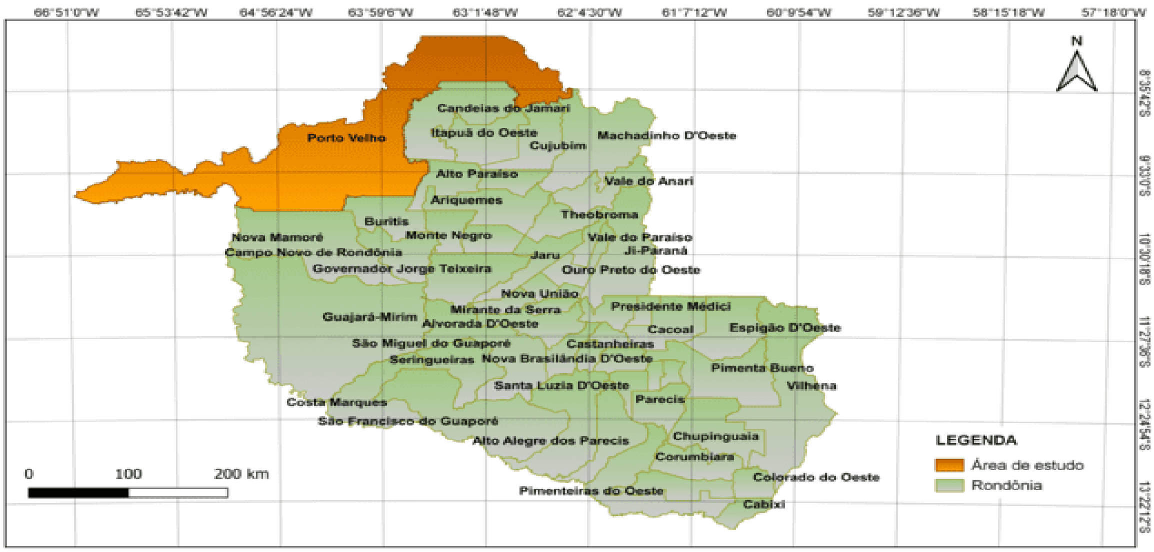

Figure 1. Location map of the study area. Source: cartographic base: IBGE (2021), SGR: SIRGAS 2000, UTM 20 S.

According to the Brazilian Institute of Geography and Statistics (IBGE), the municipality of Porto Velho has a territorial area of 34,090.952 km2. The population is estimated at 460,434 inhabitants (IBGE, 2023).

The municipality is the main access route between Manaus (AM), Rio Branco (AC) and the southern centre of Brazil and was founded around 1907 with the construction of the Madeira Mamoré Railway. The process of colonising the municipality began in 1970, stimulated by the Federal Government's tax incentive programmes with migrants from the South, Southeast and Northeast of Brazil (Silva, 2010).

Porto Velho played a direct role in the state's colonisation regime and was frequently the site of federal government settlement projects and mineral exploration. To this day, agriculture and livestock remain important economic factors in the municipality, and together with industrial activities account for around 40% of the total GDP (IBGE, 2014).

The municipality's climate is predominantly humid equatorial, meaning that temperatures are high throughout the year. The average annual temperature is approximately 25.6°C, with September being the warmest month with an average of 26.2°C and July being the coldest and driest month with an average of 24.6°C (Prefeitura de Porto Velho, 2023).

The data used for the study were Landsat 8 satellite images from the collection called 'Landsat Collection 2 Level-1', as they are a product of wide accessibility and temporal availability. According to the United States Geological Survey platform (USGS, 2023), the images available in this collection are radiometrically corrected and it was necessary to carry out an atmospheric correction. The collection chosen provides all the bands of the OLI and TIRS sensors and features data processing updates in terms of both geometry and radiometry.

The methodology comprised the following steps: 1) acquisition of images and land use maps; 2) atmospheric correction of the images; 3) conversion of the digital number of the images into top-of-atmosphere reflectance and top-of-atmosphere radiance; 4) calculation of the indices; 5) calculation of surface temperature; 6) preparation of the land cover maps for analysis;7) preparation of thematic maps for comparative analysis.

The images were acquired from the website of the USGS Earth Explorer (2023). They were selected after defining the area of interest, using their visual quality as a criterion, with cloud cover of 0%. The images selected were dated 16/07/2015 and 24/07/2018. The period established for the images was defined with the aim of monitoring the variation in surface temperature in two different years and identifying the existence of a correlation with changes in the region's vegetation cover.

The land use maps provided by the MapBiomas project, were obtained through the Google Earth Engine tool, using selection criteria such as: collection, data type, period, for the study region. The images were then saved directly to Google Drive. In order to better understand the land use processes in the municipality and then examine the relationship with land surface temperature, two land use and occupation maps were obtained for the years 2015 and 2018.

The next steps involved atmospheric correction and conversion of Digital Number (ND) into top-of-atmosphere reflectance and top-of-atmosphere radiance for the images captured by the OLI and TIRS sensors, respectively. These activities were carried out using the SCP (Semi-Automatic Classification Plugin) of the free software application QGIS v3.4. The atmospheric correction method used was Dark Object Subtraction (DOS), developed by Chávez Jr. (1988). The radiometric rescaling coefficients needed to transform ND into top-of-atmosphere reflectance or top-of-atmosphere radiance were obtained from the metadata files provided with the images. The following equations were used:

$$\rho\lambda' = M_\rho * Q_{cal} + A_P \quad (1)$$

Where:

$\rho\lambda'$: is the TOA planetary reflectance value (unitless)
M_ρ: is the multiplicative rescheduling factor in the metadata file (REFLECTANCE_MULT_BAND_X, where X is the band number)
Q_{cal}: is the digital number (ND) for each pixel.

A_P: is the additive rescheduling factor in the metadata file (REFLECTANCE_ADD_BAND_X, where X is the band number)

The TOA reflectance equation with a correction for the sun angle is given by the formula:

$$\rho\lambda = \frac{\rho\lambda'}{\cos(\theta sz)} = \frac{\rho\lambda'}{sen(\theta se)} \quad (2)$$

Where:
$\rho\lambda$: is the corrected TOA planetary reflectance.
Θse: is the solar elevation angle.
Θsz: is the local solar zenith angle (calculated from $\theta sz = 90° - \theta se$).

The spectral indices were then calculated using the bands shown in Table 1.

Table 1: Technical specifications of the OLI sensor – Landsat8

Spectral Bands	Spectral Resolution (µm)
B3 GREEN	(0,53 µm – 0,59 µm)
B4 RED	(0,64 µm – 0,67 µm)
B5 NIR	(0,85 µm – 0,88 µm)
B7 SWIR	(2,11 µm – 2,29 µm)

Source: Adaptation of USGS (2023).

The indices calculated were the Normalised Difference Vegetation Index (NDVI); Normalised Difference Wetness Index (NDWI); Normalised Burn Rate (NBR) as well as the respective difference between pre-fire and post-fire (dNBR). The indices were calculated using the QGIS raster calculator applying the equations 3, 4, 5 and 6, respectively. The result was presented in a raster file containing the values of the respective indices stored in each cell. In order to better visualise the results, it was necessary to reclassify the raster file using a standard QGIS colour palette.

The calculation of the NDVI index involves the normalised ratio between the difference and the sum of the near infrared (NIR) and red (RED) bands (ROUSE et al., 1973) and is obtained from equation 3.

$$NVDI = \frac{NIR-RED}{NIR+RED} \quad (3)$$

Where:
NIR: is the near-infrared band
RED: is the red band

The water normalised difference index was designed to delineate open water environments by automating the determination of the threshold between water and land (terrestrial vegetation and soils). The index is calculated using equation 4.

$$NDWI = \frac{GREEN-NIR}{GREEN+NIR} \quad (4)$$

where:
GREEN: is the green band
NIR: is the near-infrared band

The NBR index was developed by Key and Benson (2006) and consists of mapping burnt areas by knowing the behaviour of the spectral response in the near-infrared (NIR) and short-wave infrared (SWIR) regions. The index is calculated using equation 5.

$$NBR = \left(\frac{NIR-SWIR}{NIR+SWIR}\right) * 1000 \quad (5)$$

where:
NIR: is the near-infrared band
SWIR: is the short-wave infrared band

The measurement of fire severity is given by the difference between the pre-fire NBR and post-fire NBR (dNBR) and calculated by equation 6. To carry out this stage, two images from July 2015 and 2018 were used. A scene from July 2015 was selected to represent NBRpre and a scene from July 2018 to represent NBRpos.

$$dNBR = NBR_{pre\text{-}fire} - NBR_{post\text{-}fire} \quad (6)$$

The land surface temperature (SST) was calculated using the image corresponding to band 10 of the TIRS thermal sensor. The temperature was calculated in Kelvin and then converted into degrees Celsius for the years of 2015 and 2018 using the equations 7 and 8, respectively.

$$L\lambda = M_L * Q_{cal} + A_L \quad (7)$$

Where:
$L\lambda$: is the spectral radiance value at the top of the atmosphere $\left(\frac{Watts}{m^2 * srad * \mu m}\right)$.
M_L: is the specific scaled multiplicative factor in the metadata file (RADIANCE_MULT_BAND_X, where X is the band number)
A_L: is the specific scaled additive factor in the metadata file (RADIANCE_ADD_BAND_X, where X is the band number)

Although the sensor offers two thermal bands: 10 and 11, band 10 was used due to the uncertainties associated with the calibration of band 11, which is not recommended for this purpose (USGS, 2015).

$$T_C = T_K - 273{,}15 \quad (8)$$

Where:
T_C: is the brightness temperature in degrees Celsius (°C).
T_K: is the brightness temperature in Kelvin.

The next step was the preparation of the land cover maps, obtained using the Google Earth Engine tool, for subsequent analyses analysis. It was necessary to reproject them from the Northern Hemisphere to the Southern Hemisphere. The next step was to start reclassifying the maps, since they contained many land use and occupation classes that were not present in the region of interest, leaving only the relevant classes. This step was carried out using the QGIS tool known as ‘table reclassification’. The 3rd edition of the IBGE land use technical manual was used to help determine the new classes (IBGE, 2013).

After the reclassification, the colours of the land use and occupation classes were standardised using a file provided by the Mapbiomas project, which contains the colour font codes for each of the classes.

Likewise, a statistical report was generated of the new classes created in the previous stage, showing the approximate percentage of each one. This estimate was made using the ‘r.report’ tool, which reports statistics for raster maps, available in the QGIS software toolbox. This tool allows the user to set up a series of report parameters to be applied to a raster map and creates a standard output if output parameters is not given. The report itself consists of two parts: a) a header section; and b) the main body of the report

The header section of the report identifies the name and title oft raster map(s), project, mapset, report date, and the region of interest, described in two parts: the user's current geographic region and the mask (if any is used).

The main body of the report consists of from one to three tables which present the statistics, computed in the current geographical region, for each category and the totals for each unit column.

Finally, thematic maps were created for the months of July 2015 and 2018 of: the spectral indices presented above; land surface temperature; and land use and occupation classes. The map composer tool in the QGIS software was used for this activity. Firstly, however, it was necessary to convert the layers from matrix format to vector format in order to use the QGIS>Vector> Geoprocessing>Difference function, which aims to extract features from the input layer that are outside the output layer or partially overlap it.

Results and discussion

The results were presented through thematic maps for: spectral indices; land surface temperature; and the respective land use and occupation maps, along with detailed analyses. Additionally, synthesis maps were also developed to integrate the land use and occupation classes and land surface temperature. These maps provide valuable insights into the variety of factors associated with wildfires and their causes.

Considering that the aim of the study was to monitor the variation in land surface temperature in the municipality of Porto Velho and compare the results for July 2015 and 2018 the spectral indices were used in the study as complementary information. Since each index has a characteristic that is emphasized in the image, their use can resolve possible doubts to better discriminate the spectral response of targets in the region of interest. The Normalized Difference Vegetation Index (NDVI) better characterizes the aspect of vegetation health, while the Normalized Difference Wetness Index (NDWI) is fundamental for understanding biomass burning processes and identifying wet areas. On the other hand, the Normalized Burn Rate (NBR) better characterizes the degree of severity of fires.

Figures 2 and 3 below show the NDVI index maps for 2015 and 2018.

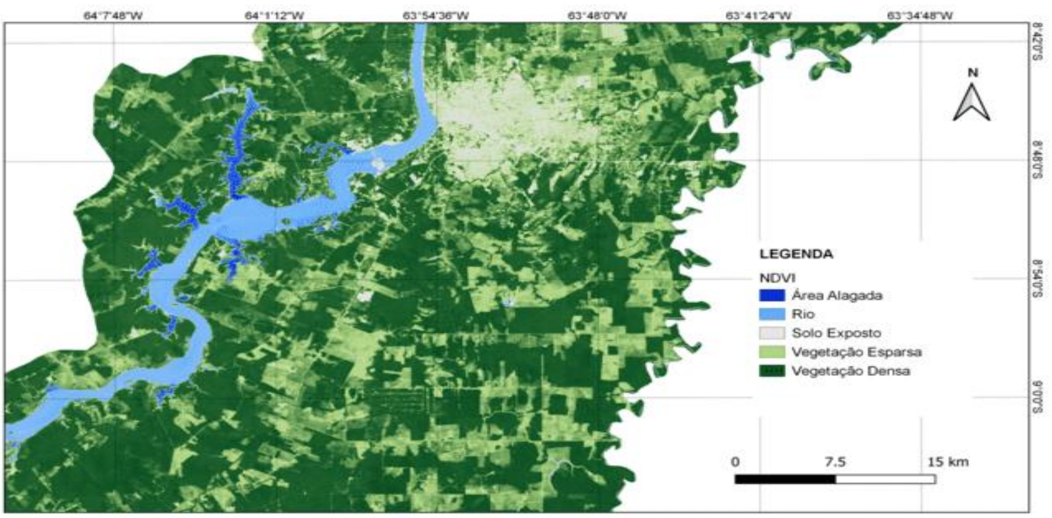

Figure 2. NDVI map for July 2015

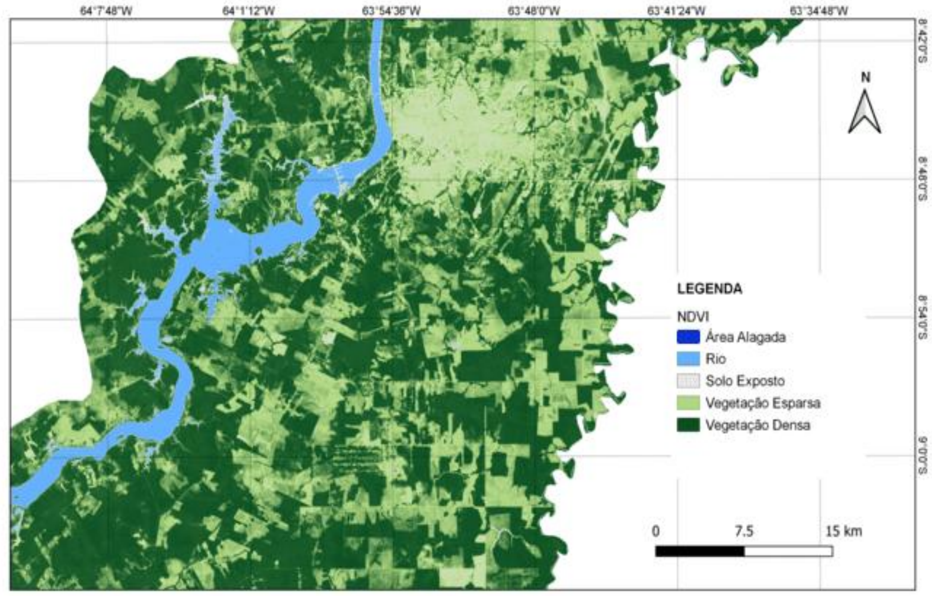

Figure 3. NDVI map for July 2018

When performing the calculation of the normalized difference vegetation index (NDVI). Values close to 1 represent areas with greater vegetation cover, represented on the map by the dense vegetation class. While values close to 0 are represented by the classes of sparse vegetation and exposed soil and indicate sick vegetation, worn out by drought or burned. On the other hand, negative values were identified as flooded areas and rivers, more specifically the Madeira River, which is the tributary of the Amazon River in the North of Brazil. This is because water reflects less in the near infrared than in the red. While areas without vegetation (exposed soil) reflect similarly in the near infrared and red, which causes the NDVI to be around zero (Dias, 2019).

According to Lotufo et al. (2020) "NDVI showed higher values in areas with dense vegetation and lower values in exposed soil, associated with dry vegetation, carbonization or with a complete absence of vegetation."

For the NDVI maps, 5 classes were adopted using the continuous mode available in the QGIS software, which pre-establishes an interval according to the values obtained. The colors adopted to represent the classes were chosen so that they were close to the reality on the ground. The main function of this index is to highlight the vegetation conditions that are associated with the aspect of vegetation cover. Therefore, as the vegetated area decreases, there is a gradual increase in surface temperature (PAVÃO et al., 2015).

According to Jensen (2009), there are two advantages of using the NDVI index. The first advantage is the possibility of monitoring seasonal and interannual changes in vegetation, as was possible to observe in the NDVI index maps and thus identify the behavior of vegetation in the municipality of Porto Velho. The second advantage refers to the reason it reduces many forms of multiplicative noise such as: cloud shadows, topographic variations and some atmospheric attenuation, present in multiple bands of images from multiple dates. Therefore, the main advantage of using this index is to monitor the vegetation cover of a region, so it becomes possible to monitor the regeneration of post-fire vegetation.

However, the NDVI index is not the most suitable for identifying burned areas, as, according to Pereira et al. (1999), there is little sensitivity to discriminate burned and unburned areas, as they present similar responses to other features, such as: sparse vegetation and exposed soil. Although the use of spectral indices, which use visible bands such as NDVI, do not demonstrate high sensitivity to the effect of fire, some authors claim that they can be useful for monitoring post-fire vegetation regeneration, as it is able to effectively differentiate areas of high and low vegetation density (Ribed & Lopez, 1995; Rebello et. al, 2020) .

Therefore, it becomes possible to generally assess the level of environmental degradation, based on the analysis of vegetation cover indices that directly classify soil protection levels through vegetation density.

Figure 4 shows the dNBR index map.

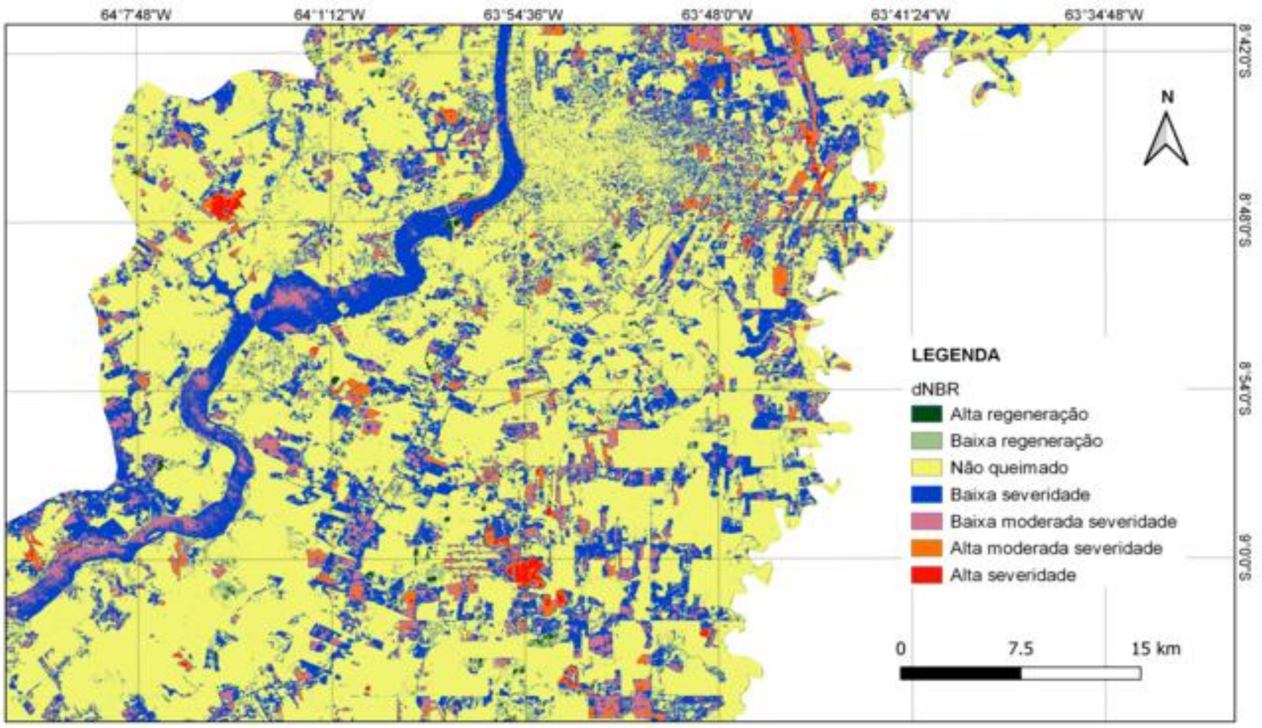

Figure 4. dNBR index map for the range July 2015 to July 2018.

The differentiated burning index by normalized ratio (dNBR) allowed, through pre- and post-fire temporal analysis, to obtain the degree of fire severity in the region of interest. It is worth mentioning that when applied to a large area and with a long time interval, the index may end up generalizing some results, due to the large number of interventions that may occur during the period. Therefore, the NBR index compares pre-fire NBR data, before the fire, and post-fire NBR data, after the fire in order to highlight the change caused by the fire (Allen & Sorbel, 2008) . Therefore, the degree of severity of fires in the municipality of Porto Velho, for the years 2015 and 2018, were represented in classes ranging from high regeneration to high severity.

The values ranged from -500 to 1300 and were grouped into 7 classes comprising the classes of high regeneration, low regeneration, unburned and low severity and showed little or no relationship with fires, while from the low moderate severity class the burned areas were better detected.

These results validate what was proposed by Miller and Thode (2007) who, when relativizing the dNBR index, found greater precision, especially for high severity fires.

The region presented some areas considered to have a high degree of severity for fires, and the main economic activity developed in the region is linked to the agricultural sector. Therefore, we can associate that these fires are the result of planting and pasture activities, as shown in the land use and occupation maps. In fact, these same areas identified in the dNBR index map, as having high severity fires, were represented by the agricultural class in the land use and occupation maps. It is common to use fire to manage some vegetation in agriculture (MISTRY, 1998). Furthermore, pasture, widely used to feed livestock, is a vegetation that easily spreads fire.

Due to the long period for a fire analysis using the index (dNBR), it is worth considering that during such a time interval, different fire occurrences may have occurred without having been captured by the index.

According to Miller and Thode (2007), accurately mapping the spatial dimension and extent of fire severity is important to recover the affected area and to understand the general patterns generated by fire.

Figures 5 and 6 below present the NDWI index maps for the years 2015 and 2018.

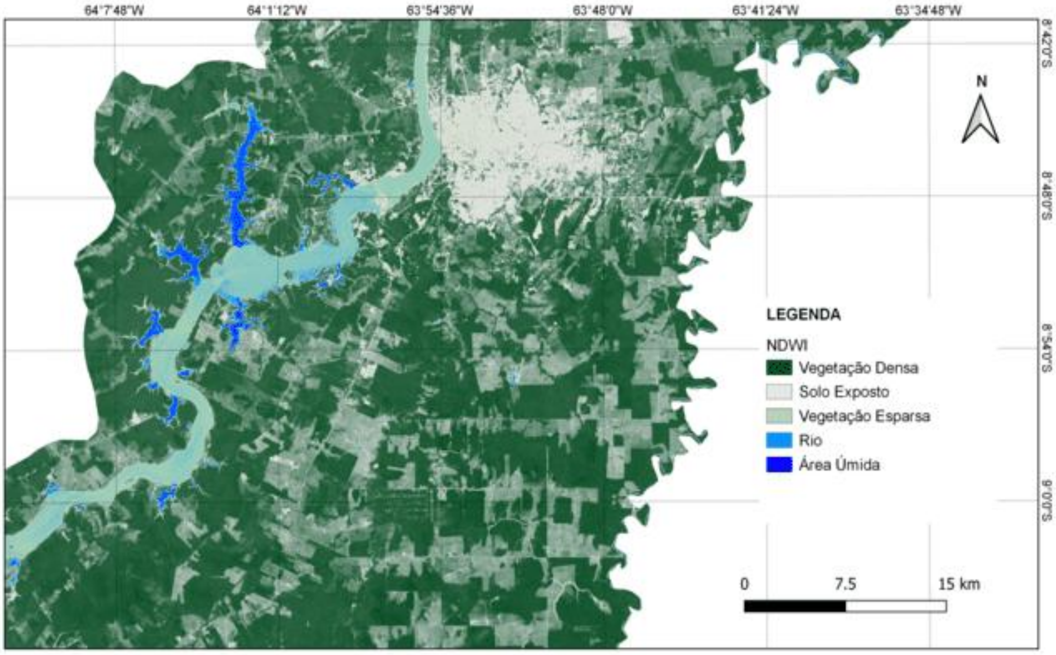

Figure 5. NDWI Map for July 2015

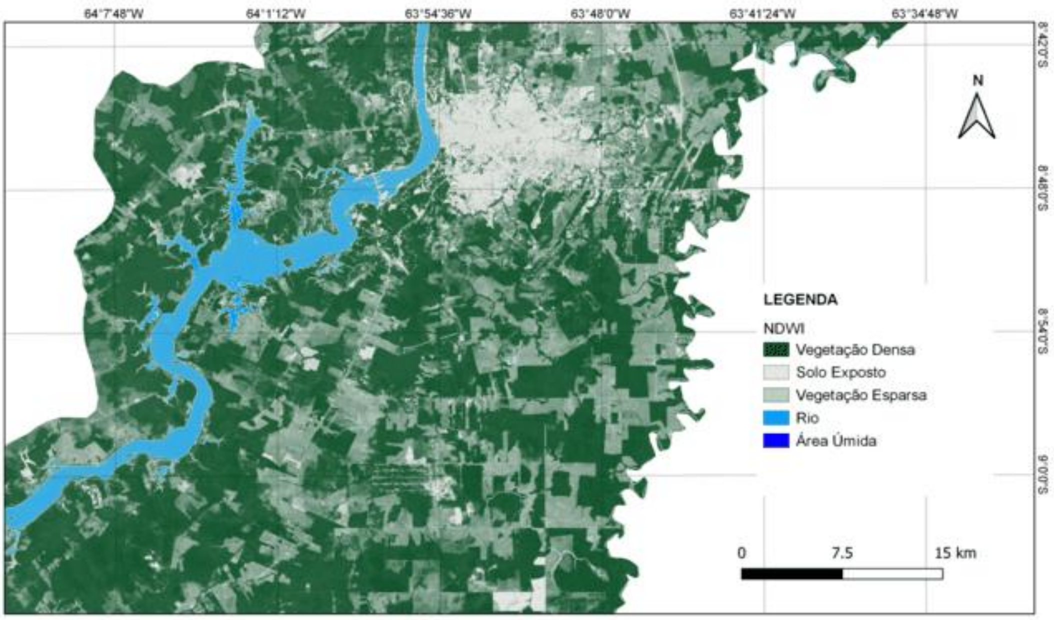

Figure 6. NDWI Map for July 2018

On the other hand, the normalized difference moisture index (NDWI) can be interpreted as an index that was derived from the NDVI, as it better highlights the features of humid areas and, in this way, allows the presence of water bodies to be identified (Leivas et al., 2013). This characteristic of the index facilitates the discrimination and interpretation of burned areas and/or humid areas. For the period established in the study, we observed that there was an expansion of the exposed soil class from 2015 to 2018.

The positive values of this index can be represented by the flooded area and river classes. As the name suggests, they indicate humid regions, that is, where there is the presence of water, while negative values are associated with classes of exposed soil, sparse vegetation or dense vegetation.

In this way, this classification made it possible to characterize and distinguish between areas of water, vegetation cover and urbanization. This index, therefore, aims to characterize regions with or without the presence of water.

In short, monitoring the variation in land surface temperature for the municipality of Porto Velho, in the years 2015 (Figure 7) and 2018 (Figure 8) in the month of July, allowed us to identify that temperatures above 30°C were presented in regions represented by classes of exposed soil or agriculture.

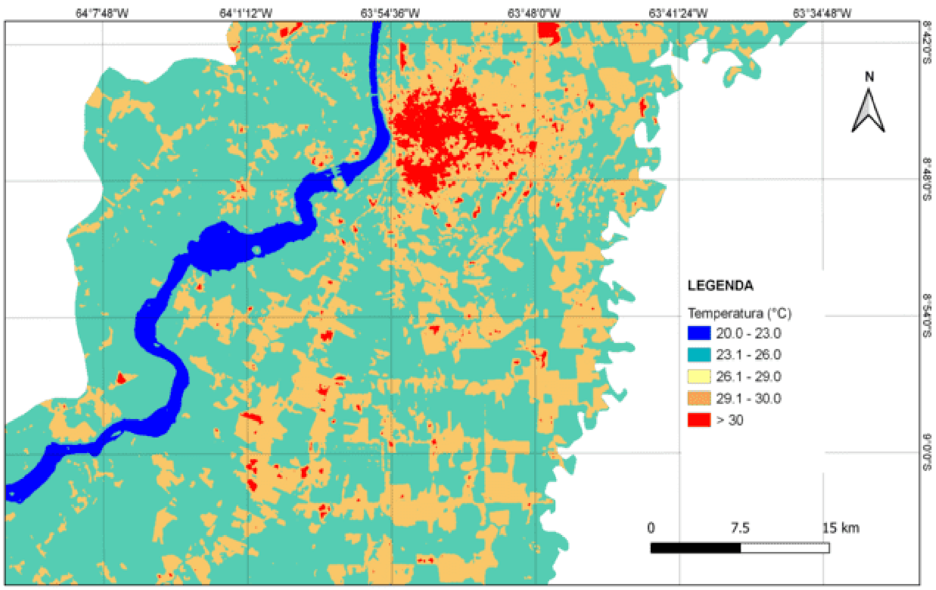

Figure 7. Land surface temperature map for July 2015.

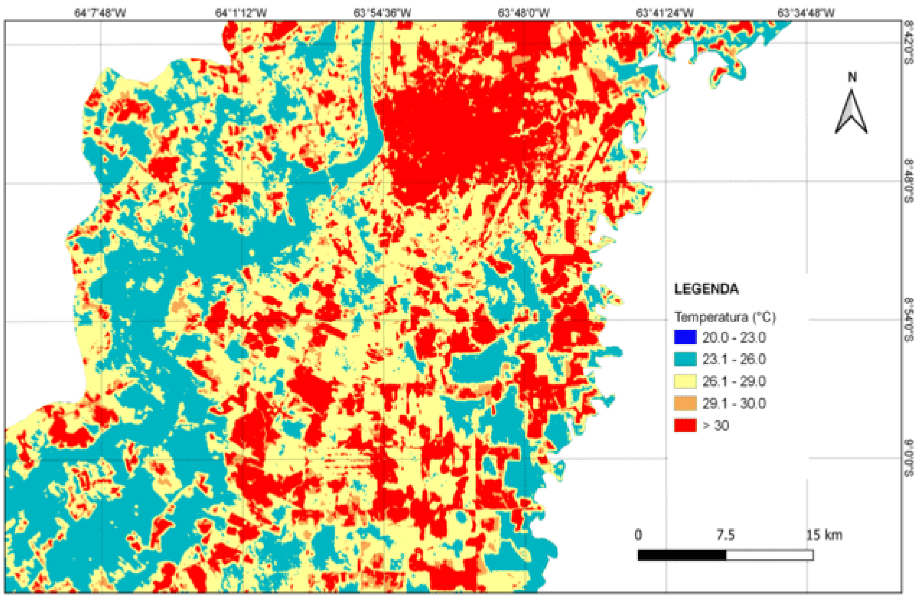

Figure 8. Land surface temperature map for July 2018.

This fact corroborates Jensen (2009) who states that deforestation and replacement of the soil surface with non-evaporative and non-porous materials, such as asphalt and concrete, directly contribute to the increase in surface temperature. Furthermore, it is worth noting that some vegetated areas also suffered from the increase in temperature, due to the type of local vegetation.

With regards to the Earth's surface temperature, one of the most immediate effects of a fire is the increase in surface temperature. In the case of an increase in local temperature, the burned surfaces absorb solar radiation more efficiently, causing an increase in the temperature of this soil (Castro Neves and Miranda, 1996), which can reach above 500°C during a short period of time, which can vary, for example, with the moisture content or the accumulation of combustible material (Dias, 1992).

Due to paved areas and due to environmental degradation there is a greater presence of exposed soil, justifying the fact that urbanized regions have high surface temperatures. Moreira & Galvíncio (2007) also commented that built areas with greater urban density (vertical and horizontal constructions), associated with the low presence of trees, contribute to the increase in local temperature.

Despite the high temperatures in urban areas, it was not possible to associate the temperature factor with the occurrence of fires for this class, since, according to what was demonstrated by the differentiated burning index by normalized ratio (dNBR), urban areas were classified as not burned. The index (dNBR) presents results focused especially on vegetation, indicating classes related to severity and regrowth. This point justifies the increase in surface temperature in vegetation areas.

Furthermore, it was found that the surface temperature and the indices are closely linked, since the higher the index value, consequently the greater the vegetation cover and the lower the surface temperature (Buyantuyev & Wu, 2009). Therefore, it is important to highlight that the highest absolute value of the index is not always associated with a higher surface temperature, as there are exceptions, such as NDVI and NDWI.

To conclude, the synthesis map aims to highlight the regions where surface temperature changes occurred for the years 2015 and 2018 (Figure 9). The areas circled in green are those that have undergone changes. It is worth noting that the algorithm identified the most significant changes, therefore, some areas where the changes were imperceptible were not located.

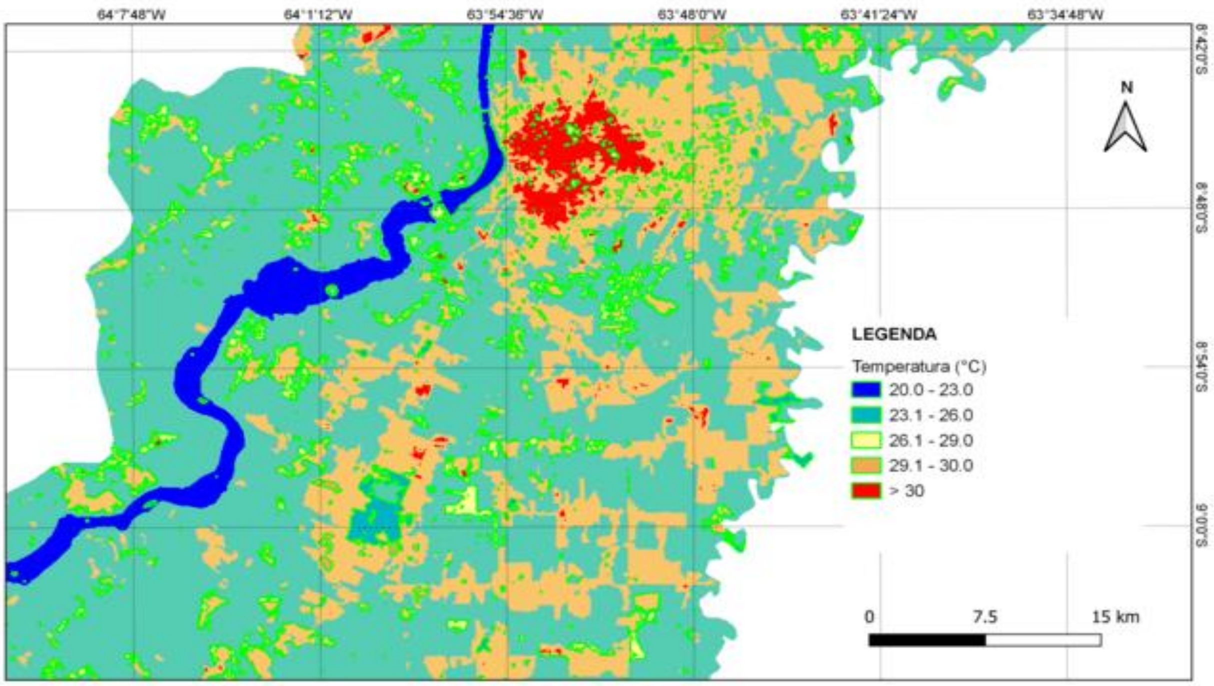

Figure 9. Summary of surface temperature variation.

The percentages of land use and occupation classes are presented in the maps below. Initially, they allowed a visual analysis of the quantity of each of the observed classes.

The synthesis map points out the vectors of transformation of land use and occupation classes (figure 12). The areas that underwent changes from 2015 to 2018 are highlighted in red. This way, you can locate the changes.

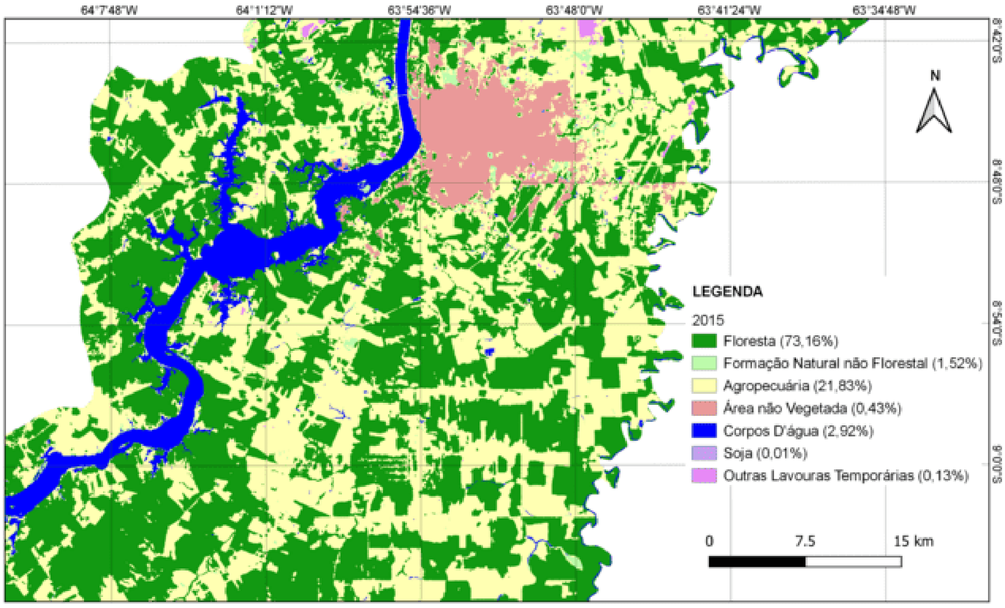

Figure 10. Land use and occupation map for July 2015, prepared based on data from MapBiomas.

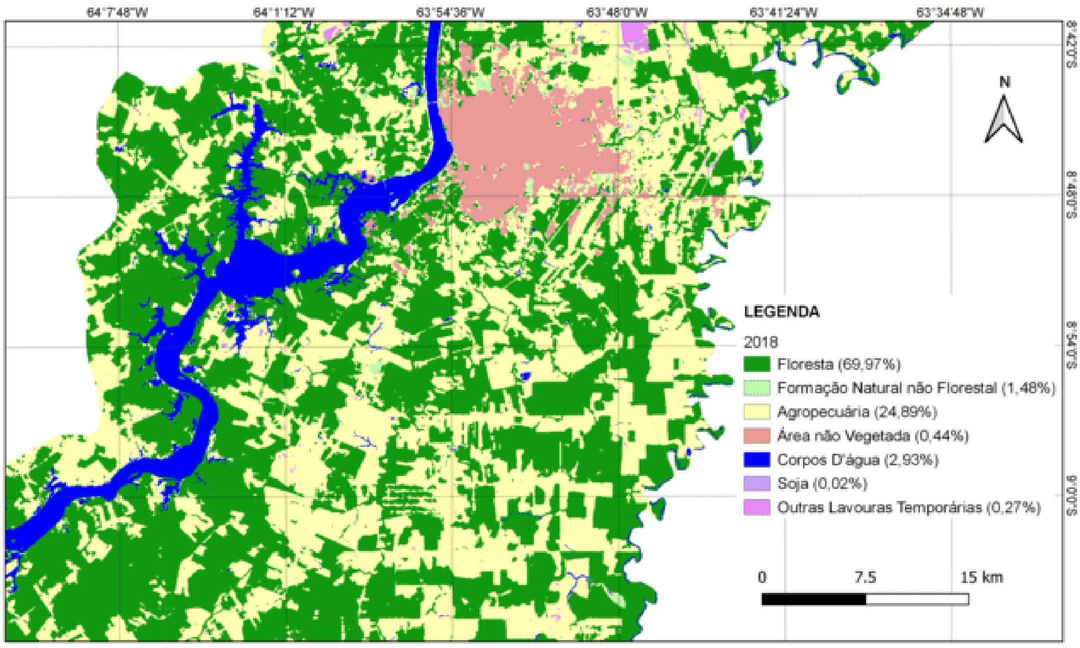

Figure 11. Land use and occupation map for July 2018, prepared based on data from MapBiomas.

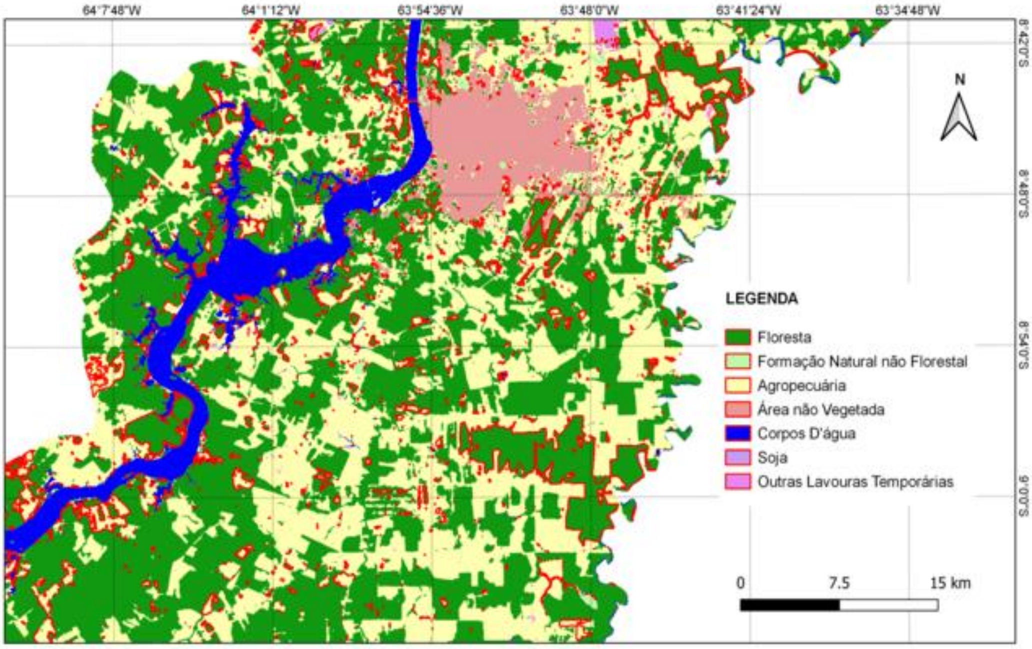

Figure 12. Synthesis of land use variation, prepared from MapBiomas data

The values obtained in percentages for the land use and occupation classes facilitate comparisons between the results of the respective years. Figure 13, below provides a comparison of the percentage of classes corresponding to the years 2015 and 2018.

```
RASTER MAP CATEGORY REPORT
LOCATION: temp_location                         Fri Jun 30 10:05:07 2023

          north: 9118389.37922926    east: 584113.10616508
REGION    south: 8892088.53586731    west:   79771.9502719
          res:        29.66712682    res:      29.66712682

MASK: none

MAP: (untitled) (rast_6536c02d9c6562 in PERMANENT)

                 Category Information                  |    %
 #|description                                          |  cover

  1| . . . . . . . . . . . . . . . . . . . . . . . . . . | 73.16
  3| . . . . . . . . . . . . . . . . . . . . . . . . . . | 21.83
  5| . . . . . . . . . . . . . . . . . . . . . . . . . . |  2.92
  2| . . . . . . . . . . . . . . . . . . . . . . . . . . |  1.52
  4| . . . . . . . . . . . . . . . . . . . . . . . . . . |  0.43
 41| . . . . . . . . . . . . . . . . . . . . . . . . . . |  0.13
 39| . . . . . . . . . . . . . . . . . . . . . . . . . . |  0.01

TOTAL                                                   |100.00
```

```
RASTER MAP CATEGORY REPORT
LOCATION: temp_location                         Fri Jun 30 10:11:24 2023

          north: 9118389.37922926    east: 584113.10616508
REGION    south: 8892088.53586731    west:   79771.9502719
          res:        29.66712682    res:      29.66712682

MASK: none

MAP: (untitled) (rast_6536c27187d563 in PERMANENT)

                 Category Information                  |    %
 #|description                                          |  cover

  1| . . . . . . . . . . . . . . . . . . . . . . . . . . | 69.97
  3| . . . . . . . . . . . . . . . . . . . . . . . . . . | 24.89
  5| . . . . . . . . . . . . . . . . . . . . . . . . . . |  2.93
  2| . . . . . . . . . . . . . . . . . . . . . . . . . . |  1.48
  4| . . . . . . . . . . . . . . . . . . . . . . . . . . |  0.44
 41| . . . . . . . . . . . . . . . . . . . . . . . . . . |  0.27
 39| . . . . . . . . . . . . . . . . . . . . . . . . . . |  0.02

TOTAL                                                   |100.00
```

Figura 13. Relatórios de classes para julho de 2015 e julho de 2018

By analyzing the percentages, it was possible to obtain information about the behavior of vegetation and land use in the municipality of Porto Velho for the years 2015 (Figure 10) and 2018 (Figure 11).

The region had 7 classes of land use and occupation, divided between: forest (73.16%); non-forest natural formation (1.52%); agriculture (21.83%); non-vegetated area (0.43%); bodies of water (2.92%); soybeans (0.01%) and other temporary crops (0.13%) for 2015. And the same for 2018, divided as follows: forest (69.97%); non-forest natural formation (1.48%); agriculture (24.89%); non-vegetated area (0.44%); bodies of water (2.93%); soybeans (0.02%) and other temporary crops (0.27%).

Thus, it was observed that the region's soil suffered from environmental effects over time, with a significant loss of local vegetation, presenting a reduction in the percentage of the forest class by approximately 3.19% from 2015 to 2018. Another relevant issue was that the agricultural sector showed an increase of approximately 3.06% from 2015 to 2018. This type of economic activity directly contributes to the increase in pasture areas and exposed soil.

The environmental impacts caused by agricultural activities arise mainly from two factors: 1) the change in land use, resulting from deforestation and the conversion of natural ecosystems into cultivated areas (Salomão et al., 2021; Alencar et al. 2021); and 2) the degradation of cultivated areas, caused by inadequate management practices. These two factors are interconnected, with the degradation of cultivated areas increasing the demand for new land for cultivation, as the cost of deforesting and incorporating new land is usually lower than that of recovering unproductive land (Gouvello et al., 2010).

Considering that the portions of land destined for production are limited, it is necessary to minimize the advance of agricultural activities over natural areas, since changes in land use produce serious impacts on the climate balance, water availability, biodiversity conservation and environmental quality (Foley et al., 2010).

In view of what was presented above, it is considered that the agricultural sector represents a cause of deforestation in the region, as these areas are used for land cultivation and animal husbandry. Associating this information with the land surface temperature and the indices, we found that for the year 2018, in which the values of the agricultural class increased and consequently those of the forestry area reduced, the region showed an increase in soil temperature.

Therefore, the values of land surface temperature, above 30°C, were more significant in the class called non-vegetated areas, that is, represented by urban regions. Vegetated areas were also greatly impacted by the increase in temperature, due to deforestation and the advance of agriculture. This concentration of high temperatures in urbanized areas exists mainly because of the predominance of asphalt and exposed soil. Furthermore, deforestation consequently reduces vegetation cover, which is essential to minimize the effects of climate and, as a consequence, there is an increase in surface temperature.

It should be noted that information on land use and occupation and land surface temperature are closely linked, as the classes represented by non-vegetated and agricultural areas were those with the highest surface temperatures. Similarly to Castillo et. al (2020) and Reis and Leal (2020), fires have taken place close to human settlements, suggesting a strong pattern of deforestation through forest fires for clearing areas and expanding peri urban zones for a variety of purposes. Knowledge about land use and occupation is essential information for a variety of social needs, ranging from natural resource management, environmental studies, urban planning, and sustainable development (Zell et al., 2012).

Finally, as a side note, it is worth noticing that due to the long period of time for analyzing fires using the index (dNBR), some fires may not have been covered by the index during this period. This article covers, however, those that have been most consistent throughout the timeframe surveyed. Nevertheless, as indicated by Costa-Saura et al. (2022) and Afina et al. (2021), it is possible to use pre-fire and post-fire NBR indices to predict fire severity in risk analysis, therefore enhancing the importance of this research as well. Therefore, the maps produced under this research may be used for risk assessment and further monitoring beyond the imagery acquisition dates.

Conclusions

Considering the various factors that determine the occurrence of fires in a location, the present study monitored the variation in land surface temperature in a region of the Amazon biome, using spectral indices and maps of land use and occupation for the municipality of Porto Velho, located in the state of Rondônia.

The vegetation indices used proved to be efficient in identifying and differentiating the vegetation cover of the studied area because they are based on the spectral behavior of the image targets.

Furthermore, it can be observed in this study that the land surface temperature and the indices are closely linked, since the higher the NDVI index value, the greater the vegetation cover of the location and the lower the surface temperature. Therefore, confirming the importance of vegetation in maintaining surface temperature.

However, NDWI results have helped in mapping and monitoring water bodies. There is no direct relationship between NDWI and surface temperature, as they are different measurements and capture different information about the Earth's surface. However, it is possible to use surface temperature data in conjunction with NDWI data for environmental monitoring studies.

On the other hand, land use and occupation maps indicated a certain incidence of areas destined for agriculture. These same areas recorded higher temperatures, drier vegetation and presented high severity values according to dNBR.

Taking into account what was exposed throughout the work, it is observed that the Differentiated Burning Index by Normalized Ratio (dNBR) is related to the increase in surface temperature and areas of drier vegetation, probably originating from agriculture.

Therefore, deforestation is related to intense urbanization processes, with transformations in soil cover, mainly due to the removal of the natural layer of vegetation and replacement with impermeable surfaces, such as concrete or asphalt, which alter the entire energy cycle of the surface, reducing and making vegetation evapotranspiration unfeasible and increasing the absorption of solar energy by the surface layer

Finally, studies on monitoring fires in the Amazon are not very common due to the impossibility of obtaining images with adequate quality to carry out the relevant analyses. This includes the absence of clouds or other types of atmospheric interference. As the Amazon biome is responsible for housing the majority of fauna and flora species, it is necessary to adopt public policies aimed at implementing environmental projects aimed at monitoring vegetation cover and consequently surface temperature.

Acknowledgement

The authors would like to thank the Department of Cartographic Engineering (CARTO) of the Faculty of Engineering (FEN) of the Rio de Janeiro State University (UERJ), for their support during the development of the work.

References

Afina, F. S., Syaufina, L., & Sitanggang, I. S. (2021). Forest and peatland fire severity assessment at Siak Regency, Riau Province using Sentinel-2 imagery. Jurnal Pengelolaan Sumberdaya Alam dan Lingkungan, 11(4), 621–630. https://doi.org/10.29244/jpsl.11.4.621-630

Alcaras, E., Costantino, D., Guastaferro, F., Parente, C., & Pepe, M. (2022). Normalized Burn Ratio Plus (NBR+): A new index for Sentinel-2 imagery. Remote Sensing, 14(7). https://doi.org/10.3390/rs14071727

Alencar, A., Castro, I., Laureto, L., Guyot, C., Stabile, M., & Moutinho, P. (2021). Amazônia em Chamas: Desmatamento e Fogo nas Florestas Públicas Não Destinadas. Nota técnica nº 7. Brasília, DF: Instituto de Pesquisa Ambiental da Amazônia.

Alencar, A., Castro, I., Stabile, M., Souza, L., Guyot, C., & Moutinho, P. (2021). Amazônia em chamas: desmatamento, fogo e pecuária em terras públicas. Nota técnica, (8), 7–8.

Allen, J. L., & Sorbel, B. (2008). Assessing the differenced Normalized Burn Ratio's ability to map burn severity in the boreal forest and tundra ecosystems of Alaska's national parks. International Journal of Wildland Fire, 17(4), 463–475. https://doi.org/10.1071/WF08010

Buyantuyev, A., & Wu, J. (2009). Urbanization alters spatiotemporal patterns of ecosystem primary production: A case study of the Phoenix Metropolitan Region. Journal of Arid Environments, 73(4), 512–520. https://doi.org/10.1016/j.jaridenv.2008.12.015

Castro Neves, B. M., & Miranda, H. S. (1996). Efeitos do fogo no regime térmico do solo de um campo sujo de Cerrado. In H. S. Miranda, C. H. Saito, & B. F. S. Dias (Orgs.), Departamento de Ecologia (ELC) (pp. 20–30). Universidade de Brasília (UnB).

Castillo, E. B., Turpo Cayo, E. Y., De Almeida, C. M., López, R. S., Rojas Briceño, N. B., Silva López, J. O., & Espinoza-Villar, R. (2020). Monitoring wildfires in the northeastern Peruvian Amazon using Landsat-8 and Sentinel-2 imagery in the GEE platform. ISPRS International Journal of Geo-Information, 9(10). https://doi.org/10.3390/ijgi9100564

Chavez, P. S. (1988). An improved dark-object subtraction technique for atmospheric scattering correction of multispectral data. Remote Sensing of Environment, 24(3), 459–479. https://doi.org/10.1016/0034-4257(88)90019-3

Costa-Saura, J. M., Bacciu, V., Ribotta, C., Spano, D., Massaiu, A., & Sirca, C. (2022). Predicting and mapping potential fire severity for risk analysis at regional level using Google Earth Engine. Remote Sensing, 14(19). https://doi.org/10.3390/rs14194812

Daldegan, G. A., de Carvalho Júnior, O. A., Guimarães, R. F., Gomes, R. A. T., Ribeiro, F. de F., & McManus, C. (2014). Spatial patterns of fire recurrence using remote sensing and GIS in the Brazilian savanna: Serra do Tombador Nature Reserve, Brazil. Remote Sensing, 6(10), 9873–9894. https://doi.org/10.3390/rs6109873

Dias, B. F. (Org.). (1992). Alternativas de desenvolvimento dos cerrados: manejo e conservação dos recursos naturais renováveis. Brasília, DF: FUNATURA.

Dias, M. B. G. (2019). Análise do índice de vegetação por diferença normalizada (NDVI) na bacia hidrográfica do Córrego do Cedro, município de Presidente Prudente, SP, Brasil. Revista de Geografia [online], 36(3). https://doi.org/10.33356/geo.v36n3

Farias, B. L., Alencar, A., Soares, F. V., & Stabile, M. (2017). Current and future patterns of fireinduced forest degradation in Amazonia. Environmental Research Letters, 12(9), 095005. https://doi.org/10.1088/1748-9326/aa69ce

Foley, J. A., DeFries, R., Asner, G. P., et al. (2005). Global consequences of land use. Science, 309(5734), 570–574. https://doi.org/10.1126/science.1111772

Gomes, R. A., Lima, R. B., & Brasil, T. V. (2024). Impacto das queimadas na Amazônia com incidência de casos de problemas respiratórios na população. Revista Foco, 17. https://ojs.focopublicacoes.com.br/foco/article/view/7057/5075

Gouvello, C., Soares Filho, B. S., & Nassar, A. (2010). Estudo de baixo carbono para o Brasil. Washington: Banco Mundial.

Hahn, M. B., Gangnon, R. E., Barcellos, C., Asner, G. P., & Patz, J. A. (2014). Influence of deforestation, logging, and fire on malaria in the Brazilian Amazon. PLoS ONE, 9(1). https://doi.org/10.1371/journal.pone.0085725

Instituto Brasileiro de Florestas (IBF). (2020). Bioma Amazônico. Disponível em: https://www.ibflorestas.org.br/bioma-amazonico. Acesso em: 20 de fevereiro de 2023.

Instituto Brasileiro de Geografia e Estatística (IBGE). (2014). Produto Interno Bruto do Município de Porto Velho.

Instituto Brasileiro de Geografia e Estatística (IBGE). (2022). Censo Demográfico 2022. Disponível em: https://censo2022.ibge.gov.br/

IPCC (Painel Intergovernamental sobre Mudança do Clima). (2024). *Mudança do clima no Brasil: Síntese atualizada e perspectivas para decisões estratégicas*. Brasília.

Jensen, J. R., & Epiphanio, J. C. N. (Coords.). (2009). Sensoriamento remoto do ambiente: uma perspectiva em recursos terrestres. São José dos Campos, SP: Parêntese.

Key, C. H., & Benson, N. C. (2006). Landscape assessment: sampling and analysis methods. USDA Forest Service, General Technical Report RMRS-GTR-164-CD.

Lotufo, J. B. S., Silva, A. G., & Santos, R. A. (2020). Índices Espectrais e Temperatura de Superfície em Áreas Queimadas no Parque Estadual do Araguaia em Mato Grosso. Revista Brasileira de Geografia Física, 13(2), 648–663. https://doi.org/10.26848/rbgf.v13.2

Leivas, J. F., et al. (2013). Monitoramento da seca de 2012/11 a partir do NDWI e NDVI padronizado do SPOT-Vegetation. In Simpósio Brasileiro de Sensoriamento Remoto.

Mayang, S., & Angraina, D. (2023). Mapping of forest and land fire hazardous using Landsat 8 satellite imagery with land surface temperature (LST) and normalized burn ratio (NBR) methods. International Remote Sensing Applied Journal, 3(2), 63–67. https://doi.org/10.24036/irsaj.v3i2.37

Moreira, E. B. M., & Galvíncio, J. D. (2007). Distribuição Espacial das Temperaturas à Superfície na cidade do Recife, utilizando imagens TM Landsat – 7. Revista de Geografia, 24(3), 122–135.

Miller, J. D., & Thode, A. E. (2007). Quantifying burn severity in a heterogeneous landscape with a relative version of the delta Normalized Burn Ratio (dNBR). Remote Sensing of Environment, 109(1), 66–80. https://doi.org/10.1016/j.rse.2006.12.006

Mistry, J. (1998). Decision-making for fire use among farmers in savannas: an exploratory study in the Distrito Federal, central Brazil. Journal of Environmental Management, 54(4), 321–34. https://doi.org/10.1006/jema.1998.0038

Nolde, M., Mueller, N., Strunz, G., & Riedlinger, T. (2021). Assessment of wildfire activity development trends for eastern Australia using multi-sensor Earth observation data. Remote Sensing, 13(24). https://doi.org/10.3390/rs13244975

Pavão, V. M., et al. (2015). Temperatura e Albedo da superfície por imagens TM Landsat 5 em diferentes uso do Solo no sudoeste da Amazônia Brasileira. Revista Brasileira de Climatologia, 16, 1–13. https://doi.org/10.5380/abclima.v16i0.43154

Pereira, A. A., et al. (1999). Spectral characterisation and discrimination of burnt areas. In E. Chuvieco (Ed.), Remote Sensing of Large Wildfires in the European Mediterranean Basin (pp. 123–138). Berlin: Springer-Verlag. https://doi.org/10.1007/978-3-642-60164-4_7

Prefeitura de Porto Velho. (n.d.). A cidade. Disponível em: https://www.portovelho.ro.gov.br/artigo/17800/a-cidade. Acesso em: 25 de fevereiro de 2023.

QGIS. (2022). Sistema de Informação Geográfica, Versão 3.4.8. Disponível em: https://qgis.org/pt_BR/site/. Acesso em: 15 de janeiro de 2022.

Reis, R. G., & Leal, M. L. M. (2020). Análise das relações de focos de calor e desflorestamento no município de Lábrea, sul do Amazonas. Planejamento e Meio Ambiente, 8(3).

Rouse, J. W., et al. (1973). Monitoring vegetation systems in the Great Plains with ERTS. In ERTS Symposium (3, pp. 309–317). NASA SP-351.

Salomão, C. S., Stabile, M., Souza, L., Alencar, A., Castro, I., Guyot, C., & Moutinho, P. (2021). Amazônia em chamas

Santana, N. C., Júnior, O. A. de C., Gomes, R. A. T., & Guimarães, R. F. (2018). Burned-area detection in Amazonian environments using standardized time series per pixel in MODIS data. Remote Sensing, 10(12). https://doi.org/10.3390/rs10121904

Silva, F. A. M. (2010). Hidrelétrica, indústria e a formação do circuito superior da economia urbana em Porto Velho (Dissertação de Mestrado, Fundação Universidade Federal de Rondônia). Porto Velho. https://repositorio.unir.br/handle/123456789/2789

Siljestroem Ribed, P., & Moreno Lopez, A. (1995). Monitoring burnt areas by principal components analysis of multi-temporal TM data. International Journal of Remote Sensing, 16(9), 1577-1587. https://doi.org/10.1080/01431169508954547

van Gerrevink, M. J., & Veraverbeke, S. (2021). Evaluating the hyperspectral sensitivity of the differenced normalized burn ratio for assessing fire severity. Remote Sensing, 13(22). https://doi.org/10.3390/rs13224611

Veraverbeke, S., et al. (2018). Hyperspectral remote sensing of fire: State-of-the-art and future perspectives. Remote Sensing of Environment, 216, 105-121. https://doi.org/10.1016/j.rse.2018.06.007

Zell, E., et al. (2012). A user-driven approach to determining critical earth observation priorities for societal benefit. IEEE Journal of Selected Topics in Applied Earth Observations and Remote Sensing, 5(6), 1594-1602. https://doi.org/10.1109/JSTARS.2012.2181333

Yao, J. Q., Zhai, H. R., Tang, X. M., Gao, X. M., & Yang, X. D. (2020). Amazon fire monitoring and analysis based on multi-source remote sensing data. In IOP Conference Series: Earth and Environmental Science (Vol. 474). Institute of Physics Publishing. https://doi.org/10.1088/1755-1315/474/4/042025